Microscopic origin of the scattering pre-peak in aqueous propylamine mixtures: X-ray and neutron experiments versus simulations

Laszlo Almasy, Alexander I Kuklin, Martina Požar, Anthony Baptista, Aurélien Perera

Microscopic origin of the scattering pre-peak in aqueous propylamine mixtures: X-ray and Neutron experiments versus simulations†

László Almásy,[a,d], Alexander I. Kuklin,[e] Martina Požar,[c] Anthony Baptista,[b] and Aurélien Perera*[b]

The structure of aqueous propylamine mixtures is investigated through X-ray and neutron scattering experiments, and the scattered intensities compared with computer simulation data. Both sets of data show a prominent scattering pre-peak, which first appears at propylamine mole fraction $x \geq 0.1$ around scattering vector $k \approx 0.2$Å^{-1}, and evolves towards $k \approx 0.8$Å^{-1} for neat propylamine $x = 1$. The existence of a scattering pre-peak in this mixture is unexpected, specifically in view of its absence in aqueous 1-propanol or aqueous DMSO mixtures. The detailed analysis of the various atom-atom structure factors and snapshots indicates that significant micro-structure exists, which produces correlation pre-peaks in the atom-atom structure factors, positive for like species atoms correlations and negative for the cross species ones. The scattering pre-peak depends on how these two contributions cancel or not. The way the amine group bond with water, produce a pre-peak through the inbalance of the positive and negative scattering contributions, unlike 1-propanol and DMSO, where these 2 contributions compensate exactly. Hence molecular simulations demonstrate how chemical details influence the microscopic segregation in different types of molecular emulsions and can be detected or not by scattering experiments

1 Introduction

When radiation, whether it is visible light, X-rays or neutrons, is scattered off a liquid, it reveals the presence of the microscopic constituents through their density correlations[1,2]. These correlations are the result of the way these microscopic constituents interact[3]. Such constituents can be atoms or molecules, but also mesoscopic objects such as micelles and monolayers, for example. For mono-atomic liquids, the scattered intensity $I(k)$ is a product of a form factor $F(k)$ describing the shape of the particle, and the structure factor $S(k)$ describing the correlation between such particles: $I(k) = F(k)S(k)$[4]. In this frequency representation, the main peak in $I(k)$ positioned at $k_M = 2\pi/\sigma$ allows to relate the mean size σ of the particles to the particle correlation peak in $S(k)$. This simple formula also holds more complex systems, such as micelles. The reason is that micelles look just like meso-atoms floating in a structureless solvent, as usually explained in various textbooks. In this case, the form factor $F(k)$ refers to the micelle shape, and $S(k)$ to micelle-micelle correlations. Since micelles are composite objects, with an underlying atomic sub-structure, the corresponding $I(k)$ will exhibit 2 scattering peaks, a main peak k_M positioned at the mean atomic size, and a pre-peak at $k_P < k_M$, related to the micelle shape and size[5,6]. Pre-peaks are equally found in neat alcohols, as $I(k)$ reveals, in addition to a main peak at k_M, their existence at $k_P \approx 0.4 - 0.7$Å^{-1} [7–9]. The origin of such pre-peak has been traced back to the existence of short chain-like clustering of the hydroxyl head groups, with mean size $d \approx 10$Å. These experimental results have been confirmed by computer simulation, both from snapshot and cluster analysis and study of the atom-atom correlation functions and corresponding structure factor[10–12]. These analyses clearly demonstrate that the pre-peak k_P is related to both the size of the chains formed in the neat liquids and their density. If one applies the same type of analysis to spherical micellar systems, for example, which are made of surfactant molecules immersed in a solution made of solvent, ions and counterions, the existence of a scattering peak around $k_P \approx 0.06$Å^{-1}is commonly interpreted in terms of spherical mi-

[a] State Key Laboratory of Environment-friendly Energy Materials, Southwest University of Science and Technology, Mianyang 621010, China ; E-mail: almasy.laszlo@wigner.mta.hu

[b] Sorbonne Université, Laboratoire de Physique Théorique de la Matière Condensée (UMR CNRS 7600), 4 Place Jussieu, F75252, Paris cedex 05, France Fax: +33 1 4427 5100; Tel: +33 1 4427 7291; E-mail: aup@lptmc.jussieu.fr*

[c] University of Split, Faculty of Sciences, Ruđera Boskovića 37, 21000, Split, Croatia

[d] Wigner Research Centre for Physics, POB 49, Budapest 1525, Hungary

[e] Frank Laboratory of Neutron Physics, Joint Institute for Nuclear Research, Dubna, Russia

celles of mean distance or size parameter $d \approx 100$Å [5,6]. Both these interpretations preserve the initial idea that a peak in $I(k)$ is related to some specific geometrical structure in the complex liquid, such as chains and spheres. Recently investigated room temperature ionic liquids (RTIL) also have a scattering pre-peak [13–16]. Indeed, these liquids are made of complex ions, which contain both charged and neutral atomic groups, and the former tend to self-associate, thus creating a mesoscopic separation between charged and neutral domains, and it is this pattern which is detected by the radiation scattering. Therefore, it would appear that the sole existence of some micro-structure in a mixture, is sufficient for a scattering pre-peak, and this micro-structure does not need to refer to any specific geometry in the self-assembled objects. However, D'Arrigo et al. have provided an exquisitely detailed investigation of aqueous binary mixtures of various short-chain alcohol molecules, such as diols and triols, some showing a pre-peak and others not [17–19]. This study does not suggest any systematic pattern between the appearance of such pre-peak and the solute shape or atomic complexity. In this context, it seems necessary to examine the details of the atomic contributions to the scattering intensity, and the simple relation $I(k) = F(k)S(k)$ is to be replaced by the very general Debye formula for $I(k)$ (see below). In the present manuscript, we report the finding of a scattering pre-peak in aqueous 1-propylamine mixtures, both from small angle X-ray (SAXS) and neutron (SANS) scattering, which appears at propylamine mole fractions above $x \geq 0.1$ at about $k_P \approx 0.2$Å^{-1}, and persists all the way to $x = 1$ into the neat solute, at about $k_P \approx 0.7$Å^{-1}. This pre-peak is unexpected, principally in view of the fact that aqueous mixtures of a similar molecule, namely 1-propanol, do not show any scattering pre-peak [20]. Since 1-propanol and 1-propylamine differ only by the hydroxyl and amine groups, it is interesting to investigate this system in order to understand the exact origin of the scattering pre-peak, particularly in terms of any underlying micro-structure. Through the use of computer simulations, we compute all the atom-atom correlations and rebuild $I(k)$, hence allowing to understand the general origin of a pre-peak in terms of the atomic details of the molecular structure of the constituents. The study helps clarify how individual atom-atom structure factors, which are the true reflectors of the underlying micro-structure, contribute to the total scattering intensity, and help or not reveal the hidden complexity of the molecular organisation.

2 Methodology

2.1 The Debye expression

The radiation scattering intensity $I(k)$ from a sample of volume V can expressed through the Debye formula [21]:

$$I(k) = \frac{1}{V} < \sum_{i,j} f_i(k) f_j(k) \exp\left(i\mathbf{k}.(\mathbf{r}_i - \mathbf{r}_j)\right) > \qquad (1)$$

where the functions $f_i(k)$ are the atomic form factor for atom i and depend on the type of radiation which is scattered, and the sum runs over all pairs of scattering atoms i,j, which are at respective spatial positions $\mathbf{r}_i$ and $\mathbf{r}_j$. The symbol <...> designates an average over all possible positions of these atoms, which could be either a thermal average in the case of experiments, or a statistical ensemble average in the case of theory and simulations. Taking into account the fact that atoms are parts of molecular species, and introducing symbols i, j to designate the molecular species index, and a_i, b_j to designate the atoms of types a and b in respective molecules and using the definition of the atom-atom total structure factor :

$$\rho\sqrt{x_i x_j} S^{(T)}_{a_i b_j}(k) = \frac{1}{V} < \sum_{m_{a_i} m_{b_j}} \exp\left(i\mathbf{k}.(\mathbf{r}_{m_{a_i}} - \mathbf{r}_{m_{b_j}})\right) > \qquad (2)$$

where the sum runs over all atoms of type a_i, b_j , and $x_i = N_i/N$ is the mole fraction of molecular species i, one could cast the equation above into the final expression which will be used herein

$$I(k) = \rho \sum_{ij} \sqrt{x_i x_j} \sum_{a_i b_j} f_{a_i}(k) f_{b_j}(k) S^{(T)}_{a_i b_j}(k) \qquad (3)$$

where $\rho = N/V$ is the number density (N is the number of particles in the volume V). It is important to understand that the total structure factor appearing in these expression contains the intramolecular atom-atom contributions, as well as those intermolecular, hence the superscript (T) for total. In the case of atoms rigidly bound inside a molecule, the intramolecular part is simply the Bessel function $j_0(kd_{a_i a_j}) = \sin(kd_{a_i a_j})/kd_{a_i a_j}$, where $d_{a_i a_j} = |\mathbf{r}_{a_i} - \mathbf{r}_{a_j}|$ is the distance between 2 atoms sites a_i and a_j belonging to the same molecule of species a. The atom-atom structure factor $S_{a_i b_j}(k)$ is related to inter-molecular pair correlation function $g_{a_i b_j}(r)$ by the formula [22]:

$$S_{a_i b_j}(k) = \delta_{ab} + \rho\sqrt{x_i x_j} \int d\mathbf{r} \left[g_{a_i b_j}(r) - 1\right] \exp(i\mathbf{k}.\mathbf{r}) \qquad (4)$$

while the total structure factor is defined as:

$$S^{(T)}_{a_i b_j}(k) = w_{a_i b_j}(k) + \rho\sqrt{x_i x_j} \int d\mathbf{r} \left[g_{a_i b_j}(r) - 1\right] \exp(i\mathbf{k}.\mathbf{r}) \qquad (5)$$

where $w_{a_i b_j}(k) = j_0(kd_{a_i b_j})$ is the intra-molecular correlation term, and the Kronecker δ_{ab} serves to discriminate unlike-species contributions. In this work, the atom-atom structure factors $S_{a_i b_j}(k)$ are computed by the Fourier transform of the atom-atom correlation function $g_{a_i b_j}(r)$ obtained from the computer simulations, and through the use of Eqs.(3,5) are related to $I(k)$, which is then compared with the experimental data obtained from X-ray and neutron scattering. As in [23], we would like to emphasize that scattering expressions neglecting the intra-molecular contributions, such as in the often cited Pings-Waser paper [24], can lead to severe underestimations of the small-k features of $I(k)$. While it is customary to mask this discrepancy by plotting $kS(k)$ versus k, such tricks do not really help spotting differences resulting from the supra-structure between the calculated and the experimental $I(k)$, which are particularly sensitive at small-k values.

2.2 Experimental and computational details

SANS experiments have been carried out at the YuMO time of flight neutron spectrometer, operating at the IBR-2 pulsed reactor [25] . Mixtures of 1-propylamine (Sigma-Aldrich, 99% purity) with D_2O have been measured at 25^{o}C in quartz cells, the scattering data corrected for transmission, scattering of the empty cell

and the incoherent background, and converted to absolute scale by comparing with scattering from vanadium, built in the instrument. The incoherent background was subtracted by measuring H_2O / D_2O mixtures with the same number density of H atoms as the studied propylamine solutions.

SAXS measurements have been performed on a SAXSpace instrument of Kratky system (Anton Paar, Austria), connected to a conventional X-ray generator (Seifert, 40kV, 50 mA, Cu K_α). Mixtures of propylamine with H_2O have been measured at 25^{o}C in standard quartz capillary of 1 mm outer diameter and 0.01mm wall thickness and the scattering was recorded by image plate in 30 min exposition times. The measured intensities were corrected for transmission, polarisation and the contribution of the empty capillary, and the data brought to absolute scale by comparing to scattering of water[26]. The data have not been corrected for the instrumental smearing[9]. The propylamine mole fraction range was 0.03-0.30 for SANS, and 0.0 - 1.0 for SAXS measurements.

The computer simulation data used in this work has been previously reported by some of us[27], and we briefly give some details. All simulations were performed with the program package Gromacs[28], with the forcefield Gromos53a6[29] for propylamine and the SPC/e[30] water. In order to properly describe the microstructure of the mixtures, a number of molecules of $N = 2048$ was found sufficient above 50% propylamine, while $N = 16000$ was found necessary for smaller propylamine concentrations. The box of neat propylamine contained 2048 particles, corresponding to the box length of 64.7 Å. As for the propylamine-water mixture, system sizes of both N = 2048 and N = 16000 were considered, yielding an average box size of 54.6 Å and 108.4 Å, respectively. These box sizes ensure that the smallest k-vector value, for which our calculated structure factors are reliable, is about 0.1Å^{-1}. The systems were simulated in the isobaric-isothermal (constant NpT) ensemble, at the temperature of T = 300K and pressure p = 1 bar, with the Nose-Hoover thermostat[31,32] and Parrinello-Rahman barostat[33]. After energy minimization, the systems were equilibrated in the NVT and then NpT ensemble, for a total of 1 ns. The following production runs lasted 4 ns, in order to sample at least 2000 configurations for calculating site-site correlation functions $g_{a_i b_j}(r)$, where a_i, b_j represent any two atomic sites on the molecules and i, j correspond to the species index.

It seems important to clarify the problems of units for various types of $I(k)$. Since the form factors have units of a distance , $I(k)$ in Eq.(3) has the dimension of an inverse length, and is usually expressed in cm^{-1}. In the case of X-ray scattering, if one uses the form factors from crystallographic tables, these are expressed in units of electron radius ($r_e \approx 2.8179$fm), hence we use the prefactor $r_e^2\rho = r_e^2(N/L^3)$ where N is the number of molecules in a simulation box of size L_B. In the case of neutron scattering, the form factors are the scattering lengths, equally expressed in femtometers, hence the prefactor is just $(1\text{fm})^2(N/L^3)$. All lenghts are expressed in cm in order to obtain $I(k)$ in cm^{-1}.

3 Results

3.1 Radiation Scattered intensities

Fig.1 shows the small angle X-ray scattered (SAXS) intensities (in cm^{-1}) from experiments and simulations, and for the various propylamine mole fractions, including neat water and propylamine.

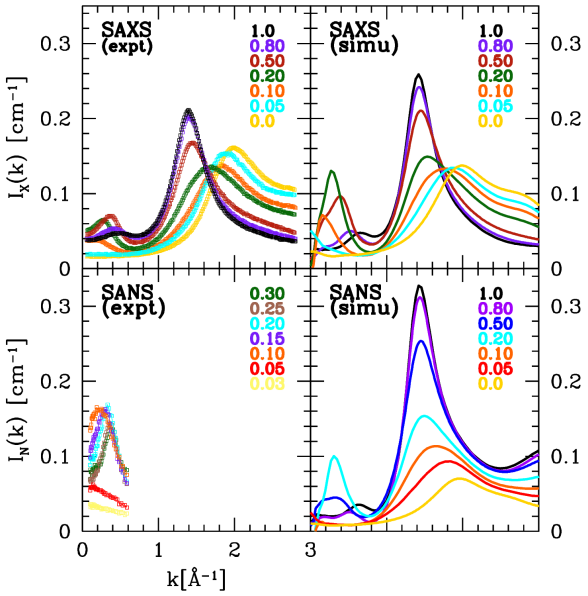

Fig. 1 X-ray and neutron scattering intensities for aqueous 1-propylamine mixtures with various propylamine mole fractions, both from experiments and computer simulations as obtained from Eq.(3). Propylamine mole fractions are displayed in each graph, with color codes associated to their respective plotted curves.

The first striking feature to be observed is the appearance of a scattering pre-peak in the overall k-range $0.2 - 0.7$Å^{-1}. The experiments show that the pre-peak appears for $x \geq 0.1$, starting at $k \approx 0.2$Å^{-1} , and moving to higher k-values as x increases. The pre-peak amplitude has a non-trivial behaviour, first increasing until $x \approx 0.2$, then decreasing. The simulation data shows exactly the same trends, both in peak positions and amplitude. But we see that the pre-peak exists even for the pure propylamine at $k \approx 0.7$Å^{-1}, predicted from both experimental and simulated $I(k)$. From this information, it is tempting to associate the scattering pre-peak in the mixture to a remnant of this neat propylamine pre-peak. We will see below that this is not the case, and that it also explains the non-monotonic bevahiour of the pre-peak amplitude with x. In any case, since this pre-peak is a collective correlation effect, it is quite remarkable that the model based simulation $I(k)$ should reproduce all the features of the real mixture spectra.

Concerning the main peak, which covers a wider range $k_M \approx 1.5 - 2.5$Å^{-1}, we observe that the characteristic peak-shoulder structure of the neat water $I(k)$, at $k \approx 2$Å^{-1} and $k \approx 3$Å^{-1}, respectively, progressively changes into a single main peak feature as the concentration of propylamine is increased, as observed in both the experimental and calculated spectra. This variation corresponds to consistently going from water molecule size $\sigma \approx 3$Å to propylamine average atomic constituent size $\sigma_{\text{eff}} \approx 4$Å, through

the use of the expression $k \approx 2\pi/\sigma$. We observe that the main peak positions are excellently reproduced by the simulation spectra. Interestingly, if we interpret the well known double peak structure of the X-ray spectra of pure water[34], as corresponding to the water-water contact at $k_{\sigma_W} \approx 2\text{Å}^{-1}$ ($\sigma_W \approx 3\text{Å}$) and the hydrogen bonding distance at $k_{HB} \approx 3\text{Å}^{-1}$ ($r_{HB} \approx 2\text{Å}$), respectively, then the dual structure is seen to persist until $x \approx 0.2$, indicating the concentrations range where the tetrahedral water hydrogen bonding holds. The observed differences in the main peak amplitudes between the experimental and the calculated intensities are a direct consequence of the united atom representation of the methyl/methylene groups of propylamine[23]. The model calculation leads to an overestimation of the carbon atom contributions, principally for the high propylamine mole fractions. While many previous investigations for several types of mixtures indicate that the agreement between simulation and wide angle scattering is generally excellent[35,36], it is not obvious that this agreement should persist in the pre-peak region. Indeed, most realistic force field models capture well correlations at contact, which explains the large-k agreement. However, the pre-peak region corresponds to the meta-molecular aggregates description, and it is not obvious that the simulations could well describe these features. The present results indicate that the microscopic details of the underlying micro-segregation are indeed well captured by model simulation, at least for this particular mixture.

Fig.1 equally shows the small angle neutron scattered (SANS) intensities from experiments and simulations. Once again, there are striking similarities between the experimental and calculated spectra, and the various pre-peak features are also consistent with SAXS results. In particular, pre-peak positions are the same. Concerning the main peak positions at $k_M \approx 1.14 - 2\text{Å}^{-1}$, we can also note similarities between the two sets of data from simulations.

To close this section, we would like to point out that the very small-k behaviour of the calculated $I(k)$ are not very accurate, and should not be taken into account. This is typically in the range $0 \leq k \leq 4\pi/L_B$, where L_B is the simulation box size. For the present simulations, this corresponds to an upper limit $k_B \leq 0.1\text{Å}^{-1}$, and values below this range should not be considered as accurate.

3.2 Snapshots

Since our simulations leads to qualitative agreement with the experimental $I(k)$, we expect that that they also represent the proper microscopic structure. Therefore, in order to understand the various origins for the pre-peaks, or their absence, we show in Fig.2 typical snapshots of the water-propylamine mixtures, for four characteristic propylamine concentrations of 5% in panel(a), 20% in panel (b), 50% in panels (c) and (d), and 80% in panels (e) and (f). For 50% and 80%, the propylamine and water are shown separately in the upper and lower panels, respectively. Through these snapshots, one might expect to observe a direct link between the micro-structure and the corresponding pre-peak structure in $I(k)$.

Fig.2a and 2b indicate that water and propylamine form segregated domains, much like what has been reported in several of our earlier papers, for aqueous mono-ols[37] and other mixtures[38,39]. For higher propylamine concentrations, we have previously reported that water tends to form chain-like aggregates[27]. In order to show this more specifically, we have explicitly shown separately water molecules (lower parts) and propylamine nitrogen groups (upper parts) for the cases of 50% and 80%. One sees very clearly water chains, and less clearly the nitrogen dimers or trimer short chains. These snapshots would suggest that the pre-peak observed for $x > 0.1$ could originate from water chain clusters, much like in neat alcohols[10,11], but also in neat propylamine[27]. But this conclusion does not apply to the 20% case, where it is clearly seen that water forms globular domains. However, a close investigation of such domains reveals that it is made of water chains juxtaposed to each others. This is entirely lost in Fig.2a for x=0.05. Although it might be tempting to associate chain-like water domains to the pre-peak, we will see below in Section 3.4 that, while water-DMSO mixtures equally show water-chains[40], there is no corresponding pre-peak in the scattered intensity[41]. It is therefore necessary to further investigate the correlations associated to the micro-structure, namely the atom-atom structure factors.

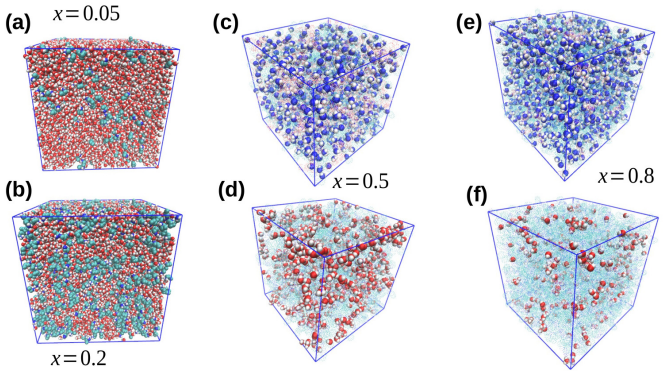

Fig. 2 Snapshots of aqueous propylamine mixtures for various propylamine mole fractions x displayed near each panels. (a) x=0.05 (for 16000 molecules); (b) x=0.2 (for 16000 molecules); (c) and (d) for x=0.5 (2048 molecules); (e) and (f) for x=0.8 (2048 molecules). For these 2 latter concentration, upper panels (c) and (e) highlight the amine groups , while lower panels (d) and (f) highlight the water molecules. Omitted atomic groups are shown as semi-transparent. In all snapshots nitrogen atoms are in blue, oxygen in red and hydrogen in white.

3.3 Structure factors

Since, as far as the simulation are concerned, it is the same structure factors which appear in the expression Eq.(3), which differs only by the atomic form factors in SAXS and SANS scattering, it is instructive to trace back the differences in the upper and lower panels of Fig.1, to features common to both of them.

To this end, we compare the various contributions of the underlying atom-atom structure factors $S_{a_i b_j}(k) = \delta_{ij} + \rho\sqrt{x_i x_j}\tilde{h}_{a_i b_j}(k)$ for the neat propylamine in Fig.3a, together with a scaled version of the SAXS intensity. One can see how the various individual atom-atom structure factors contribute to the pre-peak and the main peak, and how they get scaled down by the atomic form factors in Eq.(3). We note that all structure factors give only positive contributions. In Fig.3b, we compare the contributions of se-

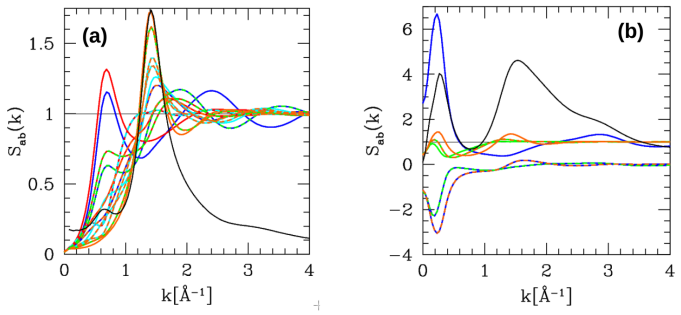

Fig. 3 (a) Atom-atom structure factors $S_{a_i a_j}(k)$ for neat propylamine from computer simulations. Like atom structure factors are shown in full lines with following color codes: nitrogen in blue, hydrogen in red, first methyl group near the amine head in cyan, second methyl in orange and last terminal methyl in green. All cross correlations are shown in dashes of the respective atom colors. The black curve is the total X-ray $I(k)$ scaled by a factor 250. (b) Selected atom-atom structure factors for the water-propylamine mixture for x=0.2. Coloring method as in (a), with water oxygen in blue, nitrogen in green and second methyl in orange. All respective cross correlations in dashed lines with the respective atom colors. The total X-ray $I(k)$ shown in black, scaled by a factor 20.

lected atom-atom structure factors for the 20% aqueous mixture, together with the corresponding $I_X(k)$, scaled to match the vertical scale. This time around, we clearly see that most like species atomic contributions give a positive pre-peak, while the cross contributions give exclusively inverse negative pre-peaks. All these contributions do not necessarily coincide at the same k-vector, but they are all about $k \approx 0.2$Å^{-1}. We also notice very clearly that it is the water structure factors which contribute mostly to the positive pre-peak. This latter finding is in stark variance with the suggestion that neat propylamine (from Fig.3a) and the 20% mixture would share the same propylamine structural features. In turn, this remark lead us to question the initial microscopic mechanisms, -i.e- the formation of short propylamine chains, that one would have in mind from the sole analysis of Fig.3a.

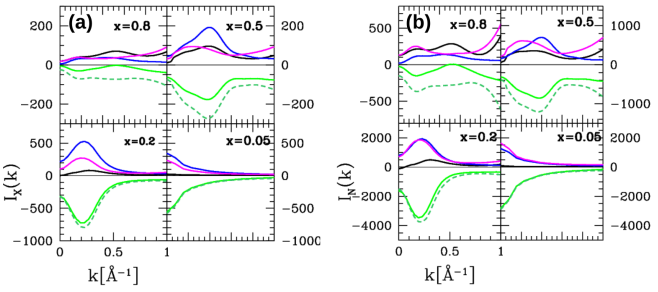

Fig. 4 Partial species-species contributions to X-ray $I(k)$ calculated from computer simulations, as defined in Eq.(6) (see text), for various propylamine concentrations x indicated in the panels. (a) for X-ray scattering and (b) for neutron scattering. $I_{ww}(k)$ shown in blue, $I_{pp}(k)$ in magenta and $I_{wp}(k)$ in green. Dashed line are explained in the text.

In order to investigate this matter further ahead, we show in Fig.4a for SAXS and Fig.4b for SANS, the various partial contributions of the species-species contribution to $I(k)$. To this end, we rewrite Eq.(3) with obvious notations as:

$$I(k) = I_{ww}(k) + I_{pp}(k) + I_{wp}(k) \quad (6)$$

and in Figs.4a-b we show the 3 contributions, $I_{ww}(k)$ for water in blue, $I_{pp}(k)$ for propylamine in magenta, and the water-propylamine cross term $I_{wp}(k)$ in green, together with the total intensity $I(k)$ in black. In addition, we show in dashed dark green the negative sum $-I_{ww}(k) - I_{pp}(k)$ of the like species contributions, with the idea in mind to see how these compensate the cross contribution $I_{wp}(k)$. We plot these contributions for 4 typical propylamine concentrations of 5%, 20%, 50% and 80%. Only the pre-peak k-range is highlighted. In each of these cases, we observe that the like species contribution is always positive, while the cross one is always negative. Comparing the light and dashed dark green curves, we see that the like species/cross species compensation is incomplete for $x > 0.2$, near complete for $x = 0.2$ and exactly compensated for $x = 0.05$. This happens both for SAXS in Fig.4a and SANS in Fig.4b, albeit with different magnitudes. These plots help understand the origin of the pre-peak in the final scattered intensities: it is the incomplete cancellation of like species and cross species contributions. However, this information by itself does not help much to understand the physical origin of the pre-peak, specifically in terms of the underlying microstructure. The only common structural feature we have found so far, is the water chain cluster pattern, that one could eventually associate to the pre-peak. To confirm, or infirm if this is true, we now compare with other aqueous mixtures we have investigated in previous works.

3.4 Other aqueous mixtures

In recent works, some of us have investigated aqueous 1-propanol[23] and aqueous DMSO mixtures[40,41]. 1-propanol is chemically more similar to propylamine than DMSO, having the same alkyl part with a hydroxyl OH head instead of an amine NH_2 head. However, our previous investigation of aqueous 1-propanol revealed very large micro-segregation, with very large domain correlation pre-peaks, positive for like species atom correlations and negative for cross species correlations, but which tend to cancel exactly to lead to a total absence of scattering pre-peak in the X-ray and neutron scattering $I(k)$, and consistent with experimental data[42,43]. We named this phenomena domain ordering correlation, by analogy with charge ordering[44]. On the other hand, our computer simulation of aqueous DMSO mixtures revealed pre-peaks in water-water structure factors, which we could attribute to the existence of chain-like water aggregates[40]. Such water aggregation appears because of the strong water-DMSO pairing, detected by many previous studies with various methodologies, which leave water molecules unable to maintain their usual tetrahedral ordering, hence enforcing chain ordering. However, this chain ordering was found not to lead to any scattering pre-peak, consistently with X-ray data, and even near excellent agreement between the computed and measured scattering intensities $I(k)$[36,41].

Both results are illustrated in Fig.5, where we show the various contributions of the scattering intensities of the 50% aqueous DMSO mixture in panel (a) and 30% aqueous 1-propanol in panel

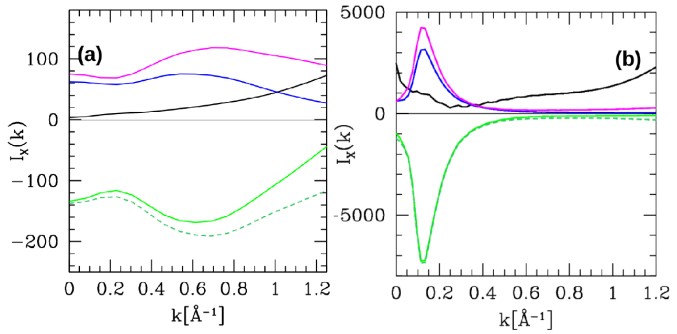

Fig. 5 Partial species-species contributions to $I(k)$ calculated from computer simulations for X-ray scattering, (a) for the equimolar aqueous DMSO mixture and (b)for 30% water 1-propanol mixture

(b), in a way similar to that shown in Fig.4. The intensities are shown in absolute (or electron) units ($I(k)/\rho$), as in Refs.[34,41,45]. The final scattering shows no pre-peak in both cases, despite the existence of a clear positive and negative pre-peaks in like and cross correlations. This result is very astonishing, mainly in view of the fact that chain clusters of the hydroxyl groups lead to a scattering pre-peak in neat alcohols and neat propylamine. This discrepancy is not currently understood and we propose an interpretation in the next section. The results of the present paper on aqueous propylamine are consistent with both aqueous alcohols and aqueous DMSO mixtures, while at the same time producing some results difficult to interpret. Indeed, we find that no scattering pre-peak is found in the domain ordering low propylamine concentration region, which is also consistent with aqueous 1-propanol results. At the same time, for propylamine concentrations higher than $x = 0.1$, we find water chain ordering, but with a scattering pre-peak, which is not consistent with what is found in aqueous DMSO mixtures, and which also show water chains. In view of the contradictory results found in neat alcohols, aqueous DMSO and aqueous propylamine, it is quite tempting not to relate the scattering pre-peak to some underlying water chain ordering.

4 Discussion

The challenge posed by the present work, is to understand the exact origin of the unexpected scattering pre-peak, seen both in SAXS and SANS as well as in the corresponding simulated spectra. We have convincingly shown that this pre-peak could not be unambiguously associated to the water chain formation witnessed in aqueous propylamine mixtures, despite the coincidental appearance of this pre-peak with the chain formation for $x > 0.1$. As mentioned in the Introduction, in scattering experiments, it is customary to associate pre-peaks with some underlying supra-molecular structure. But our previous studies have also demonstrated that, while supra-molecular structure indeed produces a pre-peak in the atom-atom structure factors, these pre-peaks come in various shapes, positive ones and inverted negative ones, associated with different types of correlations, and that their final contribution to the scattering intensity can be exactly cancelled, leading to no pre-peak. In other words, as observed in aqueous 1-propanol[23] and more recently in aqueous *tert*-butanol[46], the absence of scattering pre-peak in $I(k)$[20,47,48] does not necessarily imply the absence of micro-heterogeneity and associated structure factor pre-peaks in the $S_{a_i b_j}(k)$. Conversely, some types of micro-structure, such as chain aggregates, sometimes produce a pre-peak, as in neat alcohols, and sometimes not, as in aqueous DMSO. These differences are certainly due to the differences between the various types of solutes, which we try to rationalise now.

When comparing Fig.4 to Fig.5, one striking feature is that the water-water blue curve is below the solute-solute magenta curve for the case of no pre-peak scenario (Fig.5), whereas the ordering is reversed in Fig.5 for the cases where a pre-peak is found. We follow here the assumption that it is this inversion which is the key to explain the origin of the scattering pre-peak, and we propose a molecular picture for it. The elements provided by the simulations are that water forms chains in aqueous 1-propylamine and DMSO, while they form large globular domains in aqueous 1-propanol. Since both 1-propanol and 1-propylamine have similar number of methyl groups, we deduce that the amine group allows a better water hydrogen bonding than the hydroxyl group does, which in turn allows water to segregate much less in this latter mixture, by forming short chains instead of globular domains. This should explain why the water-water scattering contribution shows this specific inversion in these 2 mixtures, in the following way. When both species are fully micro-separated, then the species-species scattering contributions compensate exactly, whereas when the micro-separation is incomplete, the species that segregates the most (here water forming chains) contributes excedently. As to DMSO, which is known to be a rather hydrophilic molecule, the dominant solute contribution to the scattering is principally due to the large form factor of the sulfur atom. Indeed, the X-ray form factors are Gaussian-like functions[49] which start at the atomic number at $k = 0$, and this number is 16 for the sulfur atom, whereas it is 8 for oxygen, 7 for nitrogen and 6 for carbon. It is this dominance which explains why the solute-solute contribution to the scattering is above that of water. It is interesting to confront these explanations to the usual criteria for molecular hydrophobicity and hydrophilicity. Accordingly, one would select both 1-propanol and 1-propylamine as rather hydrophobic molecules (because of the dominance of the methyl groups), while DMSO would be hydrophilic[50,51]. However, these criteria alone cannot explain the inversion of the scattering curves and the existence or not of a scattering pre-peak. In addition, we note that hydrophilicity does not imply the traditional water-solute dimer picture, widely popularised in the case of aqueous-DMSO[50,51], since we find that water forms chains both in aqueous DMSO and aqueous 1-propylamine. In order to highlight the specific behaviour of water in the case of aqueous 1-propylamine, which cannot be explained neither by hydrophobocity nor by hydrophilicity, we introduce the concept of water "mingling" for this type of mixture. 1-propylamine has two hydrogens attached to the nitrogen atom, thus leading to more possibilities to water to bind to this molecule. We argue here that it is this mingling of water into the amine head group which leads both to the water chain formation and the dominant water-water scattering contribution in $I(k)$, hence leading to incomplete cancellation of like and unlike species domain correlations in favour of the like correlation, and hence the pre-peak. This argument is further

supported by the fact that, a certain amount of propylamine is required for the incomplete cancellation to happen, in other words for the water-amine mingling to occur, which is seen to happen from $x > 0.1$ both in the real and simulated systems.

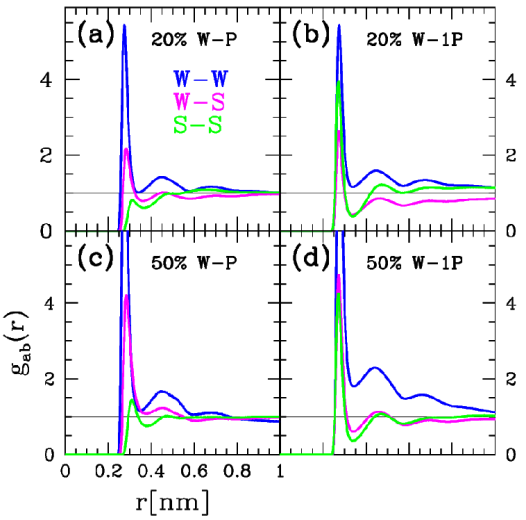

Fig. 6 Illustration of water "mingling" through comparison of hydrogen bonding sites for the case of water 1-propylamine 20% (a) and 50% (c) with water 1-propanol 20% (b) and 50% (d), respectively. $g_{\mathrm{OwOw}}(r)$ shown in blue, $g_{\mathrm{OwN}}(r)$ and $g_{\mathrm{OwO}}(r)$ shown in magenta, $g_{\mathrm{NN}}(r)$ and $g_{\mathrm{OO}}(r)$ in green.

In order to illustrate the concept of water mingling with the solute, we show in Fig.6 selected atom-atom correlation function between hydrogen bonding atoms, namely water oxygen O_w, propylamine nitrogen N and 1-propanol oxygen O. The resulting pair correlation functions are compared for the 20% solute mixtures in panel (a) and (b), and for the 50% mixtures in panel (c) and (d). All 4 panels show that the water oxygen-oxygen correlations $g_{OwOw}(r)$ are above 1, indicating that water tends to self-segregate in the distance range shown of about 1nm or so. This self-segregation is more pronounced for the water 1-propanol (panels (b) and (d)) than for water propylamine mixtures. Conversely, the comparison of the green curves show that the solute hydrogen bonding sites are more correlated at contact for the alcohol ((b) and (d)) than for the amine ((a) and (c)). This clearly illustrates that the alcohol hydroxyl groups tend to form chain-like clusters, indirectly proving that they form separated pockets. Indeed, as illustrated in our previous studies, neat alcohols tends to form better defined chains than neat propylamine[11,52]. But the most interesting features are seen in the cross correlations (in magenta). The water oxygen and propylamine nitrogen sites are clearly more correlated than for the water and alcohol oxygen sites, and this for the entire range shown. This is the definitive proof that water mingles more with the amine nitrogen than for the alcohol oxygen. In addition, this mingling happens while water tends to form segregated pockets in both mixtures and for all concentrations for which a pre-peak is seen. Interestingly, the water-solute first peak is slightly higher for the water alcohol mixtures than the corresponding water propylamine mixture. This is an indirect proof of the nature of the "interface" between the 2 components: it is more "sharp" for the water alcohol than for the water amine mixtures. These notions associated to an "interface" are to be considered with caution, since interface has a proper meaning only for a mesoscopic system, which is not the case here. Nevertheless, it helps to characterise differences in the the looseness of the segregation between different types of mixtures, hence justify the wording "water mingling" that we introduce here.

This explanation can be exported to other systems as well. For example, in neat alcohols, there no cross species correlations, and thus there is no pre-peak compensation mechanism. A very similar explanation holds also for RTILS, since the uncharged groups are attached to charged ones, the negative domain contributions are diminished. The extension of this picture to micellar systems is more involved and will be reported elsewhere. But the general idea remains the same: it is the solution-micelle "interface" which contribute mostly to the pre-peak.

A simple model can further help explain the argument above[53]. We consider a model binary mixture which micro-segregates. The pair interactions between like species 1 and 2 are simple Lennard-Jones interactions $v_{11}(r)$ and $v_{22}(r)$. The segregation can be implemented by a negative well in the cross species pair interaction $v_{12}(r)$, positioned at some large distance between the adverse molecules 1 and 2. This distance sets the domain separation. In this scenario, the positive and negative domain correlation pre-peak are exactly compensating, because of the homogeneity of the segregation throughout the system. Now, one can break this homogeneity by allowing for a mixing of species close to contact. This can be achieved by an additional attractive well in $v_{12}(r)$ superimposed to the short range interaction at contact. The effect of this well would be to increase the contact correlations, hence producing a corresponding increase of the small-k behaviour of the cross structure factor $S_{12}(k)$. This increase will counter the negative domain pre-peak, hence leading to the net positive pre-peak in the sum of the 2 contributions.

5 Conclusions

In the present study, we have studied both by traditional X-ray and neutron small angle scattering techniques, aqueous propylamine mixtures, and found the existence of a scattering pre-peak, which appears for propylamine concentrations $x > 0.1$ and persists until pure propylamine. This pre-peak is also observed in the computer simulation results, and in qualitative and near quantitative consistency with scattering experiments. The same simulations reveal the existence of chain-like water clusters for concentrations above $x > 0.1$, suggesting a link between this supra-structure and the scattering pre-peak. The detailed analysis of the atom-atom structure factor contributions reveals that this attribution is not justified, mainly in view of contradictory informations obtained in other aqueous mixtures, such as aqueous 1-propanol or aqueous DMSO mixtures. We propose that it is the presence of the amine group in propylamine which allows water to mingle with the solute, hence producing a net inbalance in the like species and cross species domain correlations, leading to a net positive pre-peak in the scattering function. This way, radiation scattering appears as a probe of the mixing behaviour of the molecular constituents. Furthermore, the explanation provides a potential

unification of the various types of scattering pre-peak in very different types if mixtures, in terms of the water-solute “interface” instead of the usual micro-structural shape explanation.

Acknowledgements

We wish to thank the support from the Franco-Hungarian BALATON No 40036PC project. MP would like to acknowledge the financial support of L’Oréal ADRIA d.o.o. together with the Croatian jury for UNESCO (the grant "For women in science").

References

1 C. Raman, *Nature*, 1923, **111**, 185.

2 B. Berne and R. Pecora, *Dynamic Light Scattering: With Applications to Chemistry, Biology, and Physics*, Dover Publications, 2000.

3 J. A. Prins, *Nature*, 1929, **123**, 908 – 909.

4 H. Fischer, A. Barnes and P. Salmon, *Reports on Progress in Physics*, 2006, **69**, 233.

5 M. Teubner and R. Strey, *The Journal of Chemical Physics*, 1987, **87**, 3195 – 3200.

6 Y. Chevalier and T. Zemb, *Reports on Progress in Physics*, 1990, **53**, 279.

7 A. Narten and A. Habenschuss, *The Journal of Chemical Physics*, 1984, **80**, 3387 , 3391.

8 S. Sarkar and R. N. Joarder, *The Journal of Chemical Physics*, 1994, **100**, 5118 – 5122.

9 M. Tomšič, A. Jamnik, G. Fritz-Popovski, O. Glatter and L. Vlček, *The Journal of Physical Chemistry B*, 2007, **111**, 1738 – 1751.

10 I. Bakó, P. Jedlovszky and G. Pálinkás, *Journal of Molecular Liquids*, 2000, **87**, 243 – 254.

11 L. Zoranić, F. Sokolić and A. Perera, *The Journal of Chemical Physics*, 2007, **127**, 024502.

12 S. Bellissima, S. De Panfilis, U. Bafile, A. Cunsolo, M. González, E. Guarini and F. Formisano, *Scientific Reports*, 2016, **6**, 39533.

13 H. Annapureddy, H. Kashyap, P. De Biase and C. Margulis, *The Journal of Physical Chemistry B*, 2010, **114**, 16838 – 16846.

14 H. K. Kashyap, C. B. Santos, H. V. R. Annapureddy, N. Murthy, C. Margulis and E. Castner, *Faraday Discussions*, 2012, **154**, 133 – 143.

15 A. Triolo, O. Russina, H.-J. Bleif and E. Di Cola, *The Journal of Physical Chemistry B*, 2007, **111**, 4641 – 4644.

16 Y. Wang and G. A. Voth, *Journal of the American Chemical Society*, 2005, **127**, 12192 – 12193.

17 G. D’Arrigo, R. Giordano and J. Teixeira, *The European Physical Journal E*, 2003, **10**, 135 – 142.

18 G. D’Arrigo, R. Giordano and J. Teixeira, *The European Physical Journal E*, 2009, **29**, 37 – 43.

19 G. D’Arrigo, R. Giordano and J. Teixeira, *Langmuir*, 2000, **16**, 1553 – 1556.

20 T. Takamuku, H. Maruyama, K. Watanabe and T. Yamaguchi, *Journal of Solution Chemistry*, 2004, **33**, 641 – 660.

21 P. Debye, *The collected papers of Peter J.W. Debye*, Interscience Publishers, 1954.

22 J.-P. Hansen and I. McDonald, *Theory of Simple Liquids*, Academic Press, Elsevier, Amsterdam, 3rd edn, 2006.

23 A. Perera, *Phys. Chem. Chem. Phys.*, 2017, **19**, 28275 – 28285.

24 C. J. Pings and J. Waser, *The Journal of Chemical Physics*, 1968, **48**, 3016 – 3018.

25 A. I. Kuklin, D. V. Soloviov, A. V. Rogachev, P. Utrobin, Y. Kovalev, M. Balasoiu, O. Ivankov, A. Sirotin, T. Murugova, T. Petukhova, Y. Gorshkova, R. Erhan, S. Kutuzov, A. Soloviev and V. Gordeliy, *Journal of Physics: Conference Series*, 2011, **291**, 012013.

26 D. Orthaber, A. Bergmann and O. Glatter, *Journal of Applied Crystallography*, 2000, **33**, 218 – 225.

27 M. Požar and A. Perera, *Journal of Molecular Liquids*, 2017, **227**, 210 – 217.

28 S. Pronk, S. Páll, R. Schulz, P. Larsson, P. Bjelkmar, R. Apostolov, M. R. Shirts, J. C. Smith, P. Kasson, D. van der Spoel, B. Hess and E. Lindahl, *Bioinformatics*, 2013, **29**, 845 – 854.

29 C. Oostenbrink, A. Villa, A. Mark and W. van Gunsteren, *Journal of Computational Chemistry*, 2004, **25**, 1656 – 1676.

30 H. J. C. Berendsen, J. R. Grigera and T. P. Straatsma, *The Journal of Physical Chemistry*, 1987, **91**, 6269 – 6271.

31 S.-u. Nosé, *Molecular Physics*, 1984, **52**, 255 – 268.

32 W. G. Hoover, *Phys. Rev. A*, 1985, **31**, 1695 – 1697.

33 M. Parrinello and A. Rahman, *Journal of Applied Physics*, 1981, **52**, 7182 – 7190.

34 G. Hura, J. M. Sorenson, R. M. Glaeser and T. Head-Gordon, *The Journal of Chemical Physics*, 2000, **113**, 9140 – 9148.

35 I. Akiyama, M. Ogawa, K. Takase, T. Takamuku, T. Yamaguchi and N. Ohtori, *Journal of Solution Chemistry*, 2004, **33**, 797 – 809.

36 E. Galicia-Andrés, L. Pusztai, L. Temleitner and O. Pizio, *Journal of Molecular Liquids*, 2015, **209**, 586 – 595.

37 A. Perera, L. Zoranić, F. Sokolić and R. Mazighi, *Journal of Molecular Liquids*, 2011, **159**, 52 – 59.

38 M. Požar, J.-B. Seguier, J. Guerche, R. Mazighi, L. Zoranić, M. Mijaković, B. Kežić-Lovrinčević, F. Sokolić and A. Perera, *Physical Chemistry Chemical Physics*, 2015, **17**, 9885 – 9898.

39 M. Požar, B. Lovrinčević, L. Zoranić, T. Primorac, F. Sokolić and A. Perera, *Physical Chemistry Chemical Physics*, 2016, **18**, 23971 – 23979.

40 A. Perera and R. Mazighi, *The Journal of Chemical Physics*, 2015, **143**, 154502.

41 A. Perera and B. Lovrinčević, *Molecular Physics*, 2018, **116**, 3311 – 3322.

42 H. Hayashi, K. Nishikawa and T. Iijima, *The Journal of Physical Chemistry*, 1990, **94**, 8334 – 8338.

43 L. Almásy, G. Jancsó and L. Cser, *Applied Physics A*, 2002, **74**, s1376 – s1378.

44 A. Perera, *Phys. Chem. Chem. Phys.*, 2017, **19**, 1062 – 1073.

45 Y. Koga, Y. Kasahara, K. Yoshino and K. Nishikawa, *Journal of Solution Chemistry*, 2001, **30**, 885 – 893.

46 S. Kaur and H. K. Kashyap, *Journal of Chemical Sciences*, 2017, **129**, 103 – 116.

47 K. Iwasaki and T. Fujiyama, *The Journal of Physical Chemistry*, 1977, **81**, 1908 – 1912.

48 K. Nishikawa, Y. Kodera and T. Iijima, *The Journal of Physical Chemistry*, 1987, **91**, 3694 – 3699.

49 E. Prince, H. Fuess, T. Hahn, H. Wondratschek, U. MÃijller, U. Shmueli, A. Authier, V. Kopsky, D. Litvin, M. G Rossmann, E. Arnold, S. Hall and B. McMahon, *International Tables for Crystallography, Vol. C: Mathematical, Physical and Chemical Tables, IUCR*, 2006.

50 A. Luzar and D. Chandler, *The Journal of Chemical Physics*, 1993, **98**, 8160 – 8173.

51 B. Kirchner and M. Reiher, *Journal of the American Chemical Society*, 2002, **124**, 6206 – 6215.

52 A. Perera, F. Sokolić and L. Zoranić, *Physical Review E*, 2007, **75**, 060502(R).

53 A. Baptista and A. Perera, *The Journal of Chemical Physics*, 2019, **150**, 064504.